A viable electrode material for use in microbial fuel cells for tropical regions

Offei, Felix; Thygesen, Anders; Mensah, Moses; Tabbicca, Kwame; Fernando, Dinesh; Petrushina, Irina; Daniel, Geoffrey

Published in:
Energies

Link to article, DOI:
10.3390/en9010035

Publication date:
2016

Document Version
Publisher's PDF, also known as Version of record

energies

MDPI

Article

A Viable Electrode Material for Use in Microbial Fuel Cells for Tropical Regions

Felix Offei [1], Anders Thygesen [2,*], Moses Mensah [1], Kwame Tabbicca [1], Dinesh Fernando [3], Irina Petrushina [4] and Geoffrey Daniel [3]

Received: 23 October 2015; Accepted: 28 December 2015; Published: 7 January 2016
Academic Editor: Chikashi Sato

1 Department of Chemical Engineering, Kwame Nkrumah University of Science and Technology, Kumasi, Ghana; felixaug4@gmail.com (F.O.); mymens14@gmx.com (M.M.); ttatotab@gmail.com (K.T.)
2 Center for Bioprocess Engineering, Department of Chemical and Biochemical Engineering, Technical University of Denmark, Søltofts Plads 229, Lyngby DK-2800, Denmark
3 Department of Forest Products, Swedish University of Agricultural Sciences, Uppsala SE-75651, Sweden; dinesh.fernando@slu.se (D.F.); geoffrey.daniel@slu.se (G.D.)
4 Department of Energy Conversion and Storage, Technical University of Denmark, Building 207, Lyngby DK-2800, Denmark; irpe@dtu.dk
* Correspondence: athy@kt.dtu.dk; Tel.: +45-2132-6303

Abstract: Electrode materials are critical for microbial fuel cells (MFC) since they influence the construction and operational costs. This study introduces a simple and efficient electrode material in the form of palm kernel shell activated carbon (AC) obtained in tropical regions. The novel introduction of this material is also targeted at introducing an inexpensive and durable electrode material, which can be produced in rural communities to improve the viability of MFCs. The maximum voltage and power density obtained (under 1000 Ω load) using an H-shaped MFC with AC as both anode and cathode electrode material was 0.66 V and 1.74 W/m^3, respectively. The power generated by AC was as high as 86% of the value obtained with the extensively used carbon paper. Scanning electron microscopy and Denaturing Gradient Gel Electrophoresis (DGGE) analysis of AC anode biofilms confirmed that electrogenic bacteria were present on the electrode surface for substrate oxidation and the formation of nanowires.

Keywords: activated carbon; palm kernel shells; nanowires; maximum power density

1. Introduction

There is an enormous need for renewable, sustainable and affordable energy resources for tropical regions in Africa, Asia and Latin America. Most of these parts of the world rely on fossil based energy sources, which make them very vulnerable to economic challenges. In order to recommend microbial fuel cells (MFC) as a viable alternative it is important that the MFC is composed of sustainable components for ease in construction, operation and maintenance.

MFCs are bio-electrochemical systems that directly convert chemical energy in organic substrates to electrical energy by the catalytic reactions of bacteria under anaerobic conditions [1]. MFCs are primarily composed of an anode and cathode separated by a proton exchange membrane. Electrogenic bacteria oxidize substrates at the anode to release electrons, protons and CO_2. Electrons are then transported through an external circuit to the cathode where they are consumed by an oxidizing agent.

Major components in MFCs are the electrodes (*i.e.*, anode and cathode), which influence microbial attachment, electron transfer, internal resistance and rate of electrode surface reactions [2]. These effects vary in different electrode materials due to differences in their physical and chemical properties.

To enhance the sustainability of an MFC, it is imperative that materials used are obtained from the same region since import and transport increases the cost greatly.

The anode electrode material requires high electrical conductivity, strong bio-compatibility, chemical stability and large surface area [3]. Carbon based materials are widely used for MFC electrodes. Power densities of 148 mW/m^2 have been recorded for carbon paper (CP) [4], 422 mW/m^2 for graphite fiber brush [5], 250 mW/m^2 for carbon cloth [6] and 2600 W/m^2 for carbon felt [7]. Challenges with the use of these materials include high prices, clogging (especially with graphite fiber brush), large resistance and fragility [8]. Modification of electrode materials by heat treatment [9] and catalysts [10] has been used by some researchers to improve electrode performance. These modifications however, represent an extra cost in the MFC reactor construction.

In previous studies, granular activated carbon (AC) was explored as anode and cathode electrode material in single chamber and double chamber MFCs [11–15]. In some of these studies, AC was used as cathode material in a composite mixture especially with Polytetrafluoroethylene (PTFE) [13,14,16], which did not explore its potential as a standalone cathode material. These studies were conducted using commercial AC material produced from coal, coconut shell and wood. Until now, there has been no study in the dual use of AC from palm kernel shells as both anode and cathode electrode material in its raw form without catalysts. The introduction of palm kernel shell AC adds a further advantage to MFCs being developed and considered for scale-up in tropical regions where palm cultivation is abundant.

Other low cost precursors such as kenaf (*Hibiscus cannabinus*) [17] and corrugate cardboard [18] have also been carbonized for use as electrode materials in MFCs but their availability and abundance in most tropical regions cannot be assured. AC production from palm kernel shell is relatively new and can become dominant in tropical regions where oil palm tree (*Elaeis guineensis*) cultivation is prominent. It is the shell fraction of nuts remaining after the palm fiber and kernel nuts have been removed following crushing in the palm oil mill. It is often used as an energy supplement due to its high calorific value of up to 18.8 MJ/kg [19] but is sometimes discarded as a waste material.

The novel use of palm kernel shells for production of AC is targeted at introducing an inexpensive (up to $2.00/kg, Department of Chemical Engineering, Kwame Nkrumah University of Science and Technology, Kumasi, Ghana) and efficient electrode material to partly replace the synthetic carbon based materials outlined above. This electrode material can be produced in rural communities and would require little education. In the AC form, palm kernel shells have high porosity, large internal surface area and high strength, which are important physical properties for an MFC [20–22]. The pore volumes have been found to 0.003–0.01 cm^3/g of mesopores and to 0.011–0.11 cm^3/g of micropores [20]. The introduction of AC is therefore very timely especially as MFCs are still in their developmental phase.

In this study, a hypothesis is put forward that a preferred choice of efficient and cost-effective electrodes for most tropical regions could be palm kernel shell AC. AC was therefore tested as electrode material in both the anode and cathode compartments of an MFC. An assessment of power generation, internal resistance and microbial community was conducted with the commonly used electrode material CP as baseline since it is successfully used in MFC research [4,8,23]. In order to obtain adequate microbial inoculation, the use of fecal sludge (FS) and grey water (GW (domestic wastewater)) were assessed.

2. Results and Discussion

2.1. Start-up and Inoculum Selection

The selected inocula FS and GW were inoculated into the anode chambers of the MFCs for biofilm formation (bacterial attachment). After 12 to 24 days of voltage-time profile observations (Figure 1), maximum voltage and power density of 0.71 V and 1.98 W/m^3, respectively, were obtained for FS after three inoculation cycles using 1000 Ω external resistance (Figure 1). The maximum voltage and power

density for GW was only 0.54 V and 1.23 W/m^3, respectively after three feeding cycles (Figure 1). Maximum voltage was obtained after six days and three days for FS and GW, respectively, in the inoculation cycle. The longer time needed with FS was mainly a result of a longer lag phase.

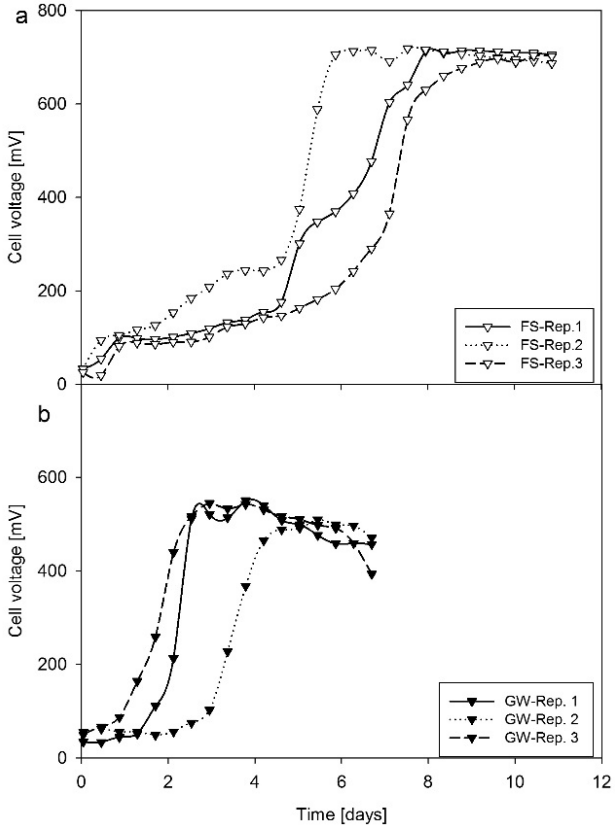

Figure 1. Selection of inoculum for microbial fuel cell (MFC) operation with carbon paper (CP) as electrode material: (**a**) CP-FS: Inoculated with faecal sludge (FS); (**b**) CP-GW: Inoculated with grey water (GW).

The high voltage produced with the FS-inoculum relative to GW could be attributed to two key factors, which included high chemical oxygen demand (COD) and solution conductivity of FS (13.1 g/L COD; 17.2 mS/cm) compared to GW (1.4 g/L COD; 1.4 mS/cm) (Table 1). The high organic loading ensured efficient substrate utilization by the mixed consortia present in the biofilm formed. The high solution conductivity favored the migration of ions in the bulk solution due to a low internal resistance. Based on the voltage and power densities obtained with FS and GW after three unique cycles of MFC operation, the most efficient inoculum was identified.

Table 1. Electrochemical impedance spectroscopy (EIS) result (R_{Ohm}), chemical oxygen demand (COD), conductivity and electrode distance determined after adding the substrate. CP forms a flat sheet while the palm kernel shell AC forms a 6 cm thick granular layer.

Electrode/Inoculum	R_{Ohm} (Total) Ω	COD (Anode) g/L	Conductivity (Anode) mS/cm	Conductivity (Cathode) mS/cm	Electrode Distance (Total) mm
CP-FS	34	13.1 ± 1.6	17.2 ± 2.4	32.0 ± 0.9	60
AC-FS	8				0 (60 mm granules)
CP-GW	158	3.6 ± 0.2	1.4 ± 0.2		60
AC-GW	34				0 (60 mm granules)

As part of the development of palm kernel shell AC as electrode materials for MFCs, a careful observation of its inoculation was critical since without a biofilm there would be little or no electricity

generation. AC was used as electrode material in both anode and cathode of the MFCs supported by a stainless steel rod as electron collector to the external circuit.

The inoculation of palm kernel shell AC yielded a maximum voltage and power density up to 0.60 V and 1.44 W/m^3 (AC-FS), respectively (cycle 1; Figure 2) and was successful due to the stable power and voltage obtained in cycle 1. The electron transfer can be considered as microbial induced since the initial voltage (day 1) when biofilm was absent was negligible.

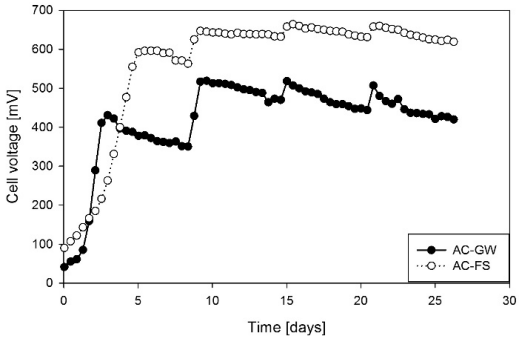

Figure 2. Electricity generation of MFCs operated with palm kernel shell activated carbon (AC) as electrode material testing FS and GW as inocula.

2.2. Electricity Generation from Palm Kernel Shell AC

The generation of electrical energy is the primary purpose of MFC research with the electrode materials in the anode and cathode playing a critical role. The selection and development of AC was targeted at introducing a cost-effective electrode material for use in MFCs. The successful inoculation of AC indicated that an improvement in power generation can be achieved through post-inoculation cycles [24,25]. Numerous cycles of operation are known to improve biofilm and increase the total power generated. In each post-inoculation cycle, fresh substrate was added to the anode. Cycles 2, 3 and 4 show that a significant increase in maximum power was achieved (9%–17%) compared to that recorded during the inoculation in cycle 1 (Figure 2).

The three post-inoculation cycles yielded an average maximum voltage of 516 $\pm$ 7 mV for AC-GW and 657 mV $\pm$ 8 mV for AC-FS. The power densities obtained were 1.07 $\pm$ 0.03 W/m^3 for AC-GW and 1.73 $\pm$ 0.05 W/m^3 for AC-FS. Steady voltage above 0.6 V was available for the entire cycle time (six days) in all three post inoculation cycles for FS operated MFCs. However, steady voltage (*i.e.*, >0.6 V, Figure 2) attained for FS was presumably due to its higher COD content than GW, which enhanced substrate availability and utilization by electrogenic bacteria (Table 1). A good inter-granular electron transfer was also achieved as evident in the stable and appreciable overall voltages obtained under the 1000 Ω load (Figure 2). Especially with FS, stable performance was obtained for at least 25 days.

2.3. Electrochemical Interpretation of Resistance from the EIS Data

Nyquist plots (Figure 3) were generated using electrochemical impedance spectroscopy (EIS) with the aid of a potentiostat to determine the overall internal resistance (impedance). The impedance (R_{Ohm}) was determined as the x-intercept on the real impedance axis, Z_{real} of the plot (Figure 3) and is shown in Table 1. An overall R_{Ohm} of 31 $\pm$ 4 Ω was measured for AC-GW MFCs and 7.5 $\pm$ 1 Ω for AC-FS MFCs. R_{Ohm} in the MFCs with palm kernel shell AC were fairly consistent in all cycles of FS and GW operated MFCs. GW operated MFCs recorded a 4.5 times higher R_{Ohm} than with FS due to its low anode solution conductivity (Table 1). The explanation is that the high solution conductivity favored the proton transfer. The effect of R_{Ohm} in the AC-GW MFCs is visible in its lower power output. With CP, R_{Ohm} was 4.6 times larger, which is due to the electrodes being 60 mm away from each other, while some palm kernel shell AC-granules were only 0–5 mm apart giving a low R_{Ohm} (Table 1).

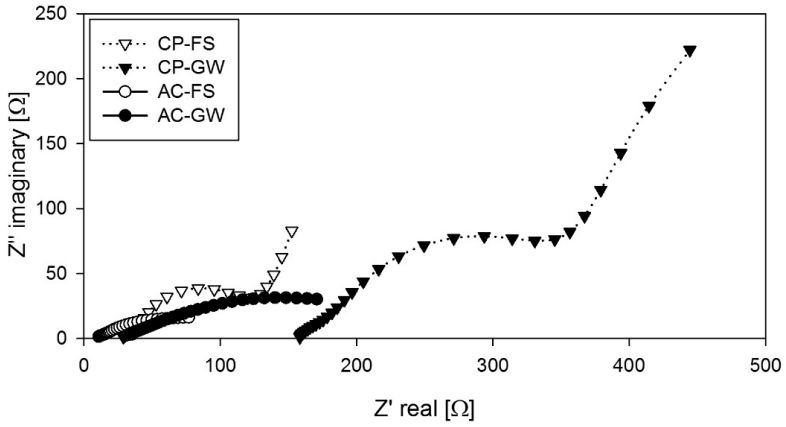

Figure 3. Nyquist plots of overall MFC impedance from CP and palm kernel shell AC determined by EIS.

EIS was thereby a fast and useful technique for evaluation of the electrode materials and the inocula. Considering the whole curves shows: CP-GW: It can be assumed that it is bounded Warburg impedance diffusion (45° angle). CP-FS: Same case but lower capacitance contribution observed as lower resistance. Palm kernel shell AC has lower impedance since a part of the granules are close to each other and has a more complicated structure. Furthermore, the space surrounding the granules forms a porous electrode resulting in a depressed semicircle. AC-FS: Due to the above reasons, the lowest impedance was obtained [26].

2.4. Microbial Analysis of CP and AC Biofilms

The anodic biofilms in the MFCs were sampled at the end of the inoculation cycles for 16S ribosomal DNA (rDNA) coding for the 16S ribosomal RNA. Denaturing Gradient Gel Electrophoresis (DGGE) analysis was subsequently conducted in combination with a marker to identify the bands on the resulting polyacrylamide gel. The DGGE band patterns of samples analyzed are shown in Figure 4 and their gene bank matches indicated in Table 2. A marker containing similar rDNA-bands from five known bacterial species isolated from a CP biofilm [25] was used as reference to identify the electrogenic species present in biofilms from CP (FS and GW inoculations) and palm kernel shell AC (FS and GW inoculations). The bacterial species found in CP-FS and CP-GW anodic biofilms were similar and included *Geobacter sulfurreducens*, *Enterobacter cancerogenus*, *Thermanaerovibrio acidaminovorans* and *Desulfuromonas acetexigens*. Bacterial species found in AC biofilms also included *G. sulfurreducens*, *E. cancerogenus* and *D. acetexigens*. In the MFC study by Sun *et al.*, all the identified bacteria except *D. acetexigens* were identified, which indicates a large similarity in the microbial community due to the use of wastewater, even though the inocula have been obtained from Denmark, Europe in that study [24].

Table 2. 16S rDNA denaturing gradient gel electrophoresis (DGGE) gene band identification and characterization of the bacterial species.

Band	Accession Number.	Gene Bank Match	Identity (%)	Characteristics [24,25]
1	LN651003	*Thermanaerovibrio acidaminovorans*	87	Thermophilic anaerobe fermenting amino acids.
2	LN651037	*Shigella flexneri*	99	Facultative anaerobe.
3	LN651020	*Enterobacter cancerogenus*	99	Glucose fermenting anaerobe.
4	LN651027	*Geobacter sulfurreducens*	99	Metal-reducing anaerobe oxidizing short-chain fatty acids able to generate electricity.
5	LN650991	*Desulfuromonas acetexigens*	98	Obligate anaerobic and sulphur-reducing eubacterium oxidizing acetate as carbon resource.

G. sulfurreducens identified in both CP and AC biofilms is a well-known electrogenic species in MFCs for direct electron transfer (*i.e.*, belonging to a dissimilatory metal reducing bacterial group). The mixed culture identified in the anode biofilms are involved in symbiotic breakdown of organic compounds for enhanced oxidation by other electrogenic species incapable of direct organic substrate breakdown. *T. acidaminovorans* is known to ferment amino acids and *E. cancerogenus* for fermenting glucose to volatile fatty acids for further oxidation by electrogenic species. The identical DGGE band patterns for FS and GW can be traced to the original source and composition of the samples. GW was composed of wastewater from laundries and washrooms while FS was mainly composed of fecal matter from washrooms and urinals. The similarities in bacteria identified were therefore due to the fecal matter present in both sources.

The Shannon diversity index (H) measures the variability of the microbial community with regards to number of species (S) and their abundance as presented in Table 3. Pielou species evenness reflects the similarity of the communities. The species richness ($d = (S - 1)/\ln N$) is explained as number of species relative to population size [27]. The number of identified species was highest for FS as inoculum (10–16 DGGE bands) and highest for CP electrodes (14–16 DGGE bands) (Table 3). The high population size resulted in higher Margalef richness of 1.95–2.15 for CP compared to 0.94–1.44 for AC (Table 3). However the community was very even with respect to both inocula and electrode materials with a Pielou species eveness of 0.97–0.98. This resulted in largest Shannon diversity index for CP-FS (2.70) compared to AC-GW (1.91) (Table 3). This can be explained from the highly diverse microbial community found in FS compared to the more diluted GW. A larger and even community was thereby obtained with the CP.

Table 3. DGGE results including number of bands, Shannon diversity index, Margalef species richness and Pielou species evenness [15,28].

Electrode Material	Palm Kernel Shell AC		CP	
Inoculum	FS	GW	FS	GW
DGGE Bands (S)	10	7	16	14
Shannon diversity index (H)	2.24	1.91	2.70	2.56
Margalef species richness (d)	1.44	0.94	2.15	1.95
Pielou species evenness	0.972	0.980	0.972	0.969

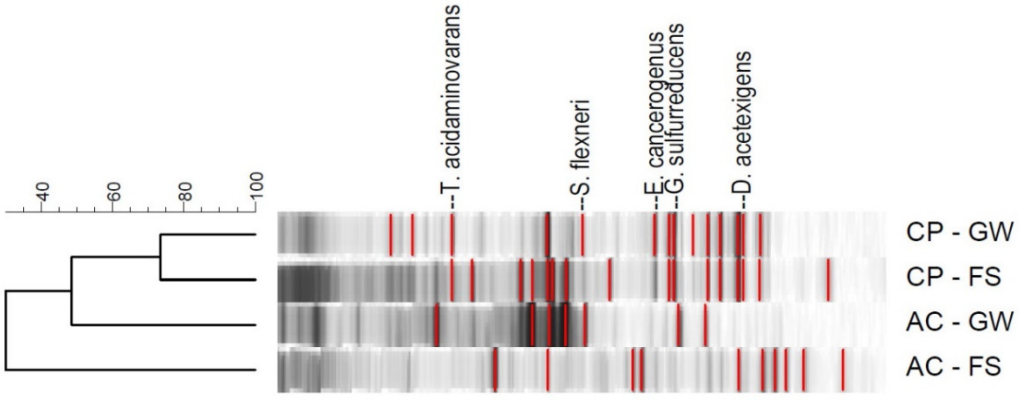

Figure 4. DGGE gel band image for the analyzed electrode biofilms (horizontal labels indicate the biofilm samples for CP and palm kernel shell AC inoculated with GW and FS.

2.5. SEM Analysis of Electrode Biofilm

The surface micro-structure and biofilm adhesion on the electrodes (CP,AC) were studied using SEM and representative micrographs are shown in Figures 5 and 6. SEM observations showed the original CP surface to consist of a structured network of carbon strands providing an extensive

surface area for attachment of microbial material (Figure 5a). Surfaces of the carbon strands were very smooth and clearly visible (Figure 5b) and the interconnected network of strands created macro- and micro-porous structure within a CP. Figure 5a,b are used as representative control images for showing changes caused by FS and GW biofilm development.

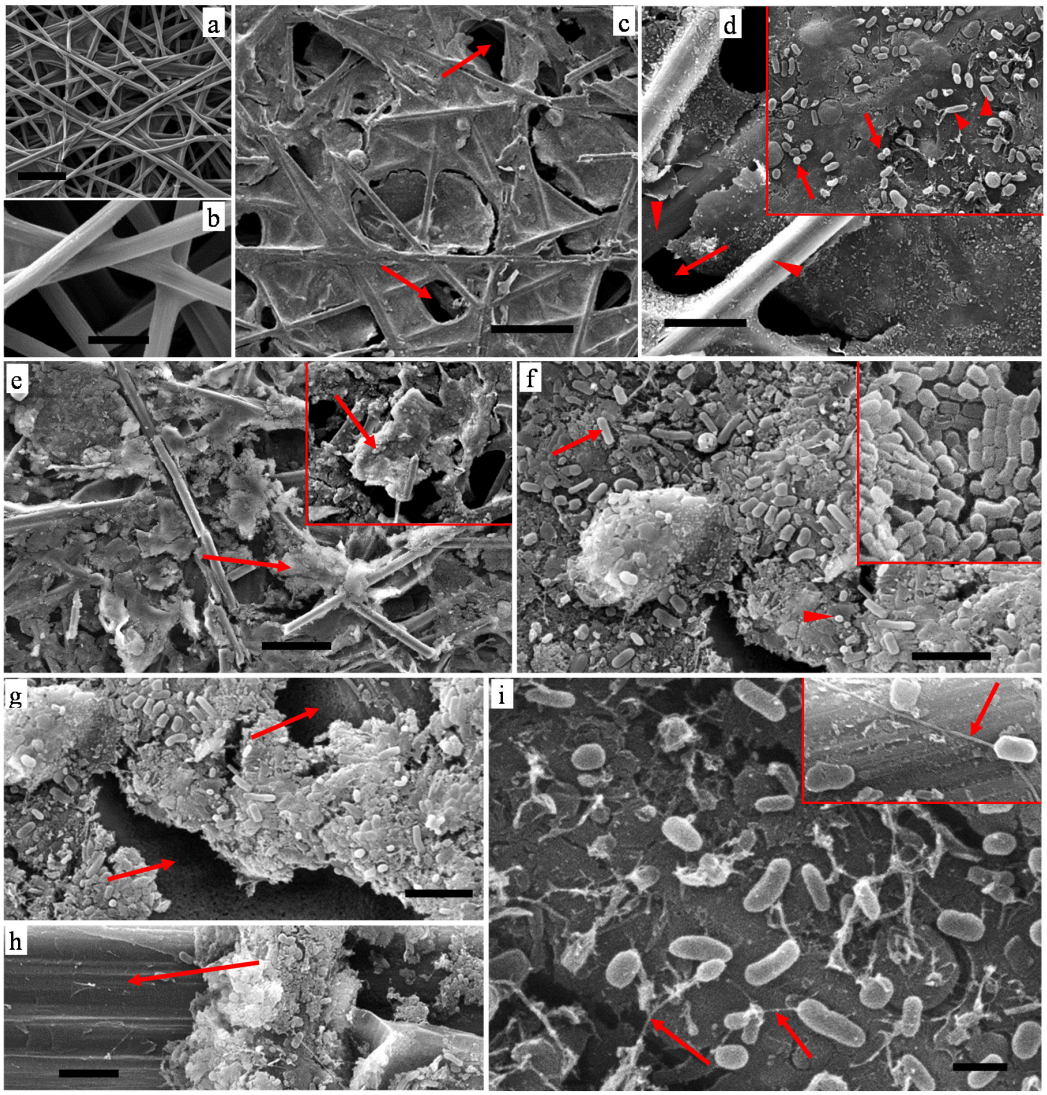

Figure 5. Scanning electron micrographs (SEM) of CP biofilms: (**a**,**b**) CP before inoculation showing interconnected network of smooth carbon strands; (**c**,**d**) CP-GW inoculation; (**e**–**i**) CP-FS inoculation. Bars: a,c, 100 µm; b,d, 20 µm; e, 50 µm; f,g,h, 5 µm; i, 1 µm.

The biofilm structure developed on CP-GW anodes consisted of thin organic tissues irregularly distributed (Figure 5c,d). The organic tissues which appeared as a discontinuous film over the carbon strands (arrows in Figure 5c,d) were embedded with bacteria (Figure 5d) with both bacillus (rod-like; arrowheads, inset top right) and cocci (spherical; arrows, inset top right) forms. Bacteria were seldom observed in areas where no organic tissue/film was present (arrowheads, Figure 5d).

The biofilm structure of CP-FS anodes was also composed of organic tissues covering the inter strand network (Figure 5e). However, in contrast to GW, the organic tissue in the FS biofilm appeared rather thick and dense with large particles over the carbon strands (arrows in Figure 5e and in inset top right). The biofilms were composed of highly populated bacterial forms (Figure 5f) sometimes packed densely and attaching to each other (Figure 5f, inset top right).

The bacteria were dominated by bacillus types (Figure 5f, arrow and inset) along with some cocci forms (Figure 5f, arrowhead). As observed with CP-GW, bacteria on CP-FS electrodes were strongly associated with organic materials and no or very little bacteria were observed on smooth surfaces of the CP where no extraneous particles (e.g., organic materials) were present (arrows in Figure 5g,h). This indicates a relation between bacterial activity and abundance of organic materials within an electrode. It is notable that *Geobacter* sp. belongs to the bacillus group of bacterial forms [29]. Furthermore, pilus-like surface appendages (nano-thread-like) ranging from 50–120 nm in width and extending sometimes tens of μm in length (Figure 5i, inset) were observed associated with rod-shaped bacteria (arrows, Figure 5i) presumably representing bacterial nanowires. They were found associated with biofilms from both anode types but more frequent on CP-FS.

The most significant feature of the biofilms from the two anodes was the density of the film, with FS biofilms being denser than GW biofilms, which was due to the abundance of organic materials. Since the denser biofilm performed best in the MFC, a correlation can be inferred between biofilm density and performance. The SEM images for both FS and GW anodes provide evidence for development of biofilm on the electrode surface, which is known to initiate substrate oxidation for the release of electric current.

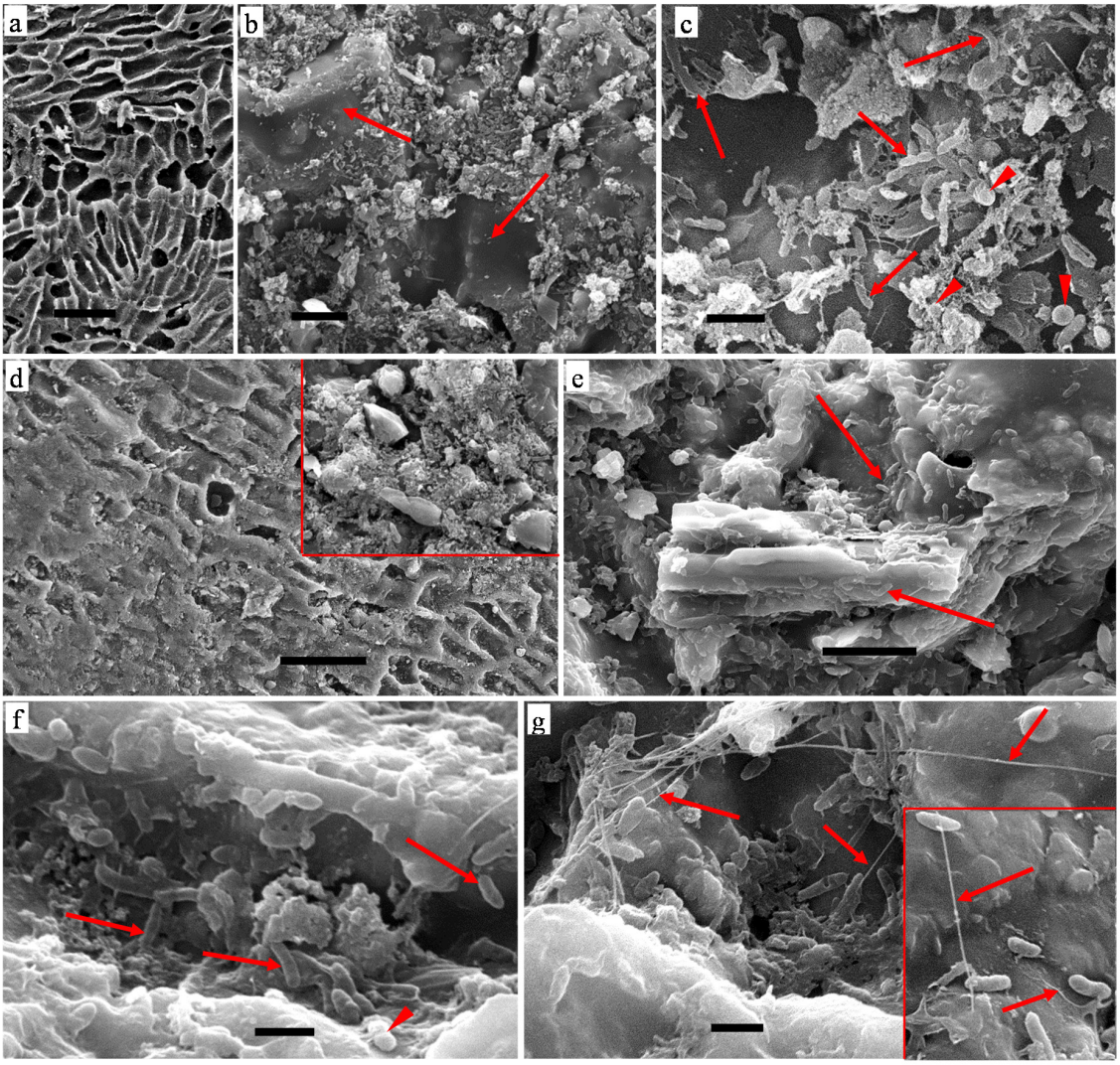

Figure 6. SEM micrographs of palm kernel shell AC biofilms: (**a**) AC before inoculation showing surface micro-structure after steam treatment; (**b**,**c**) AC-GW inoculation; (**d**–**g**) AC-FS inoculation. Bars: a,d, 50 μm; b,e, 10 μm; c,f,g, 2 μm.

SEM observations on the surface structure of palm kernel shell AC granules before inoculation and characteristics of the biofilms developed are shown in Figure 6. The AC granules surface were laden with micro-porous networks caused by the steam treatment phase of their production (Figure 6a). The porous surface was conducive for bacterial attachment for the formation of biofilm as seen in Figure 6e,f. In addition, the varied morphological structure of the AC granules would enhance their surface area for biofilm development. Figure 6b,c show AC-GW with fragmented organic tissue as its biofilm; the organic materials were sparsely distributed over AC granules with no other organic materials present (arrows in Figure 6b). A diverse population of bacterial forms deposited in the tissues includes different types of rod-like and cocci forms (arrows and arrowheads respectively in Figure 6c), dispersed thinly presumably due to the limited abundance of organic tissues.

Figure 6d–g, show representative images of AC inoculated with FS, with dense particles which are possibly rich in organic substances (Figure 6d, inset) covering the micro-porous surface (Figure 6d). Biofilm micro-structure of AC-FS consisted of a greater bacterial population (Figure 6e,f) most likely related with the abundance of organic materials similar to the SEM observations on CP-FS. Bacterial forms embedded in the organic tissues (Figure 6e, arrows) were of bacillus and cocci forms with the former being dominant (arrows and arrowhead respectively in Figure 6f). Extracellular appendages most probably representing bacterial nanowires were also observed associated and connecting the bacillus form (arrows in Figure 6g and in inset). *G. sulfurreducens* produces highly conductive nanowires and have potential for long-range exocellular electron transfer across biofilm via intertwined nanowires [30]. Results from SEM observations on AC thus showed similar characteristics to CP, with a surface providing bacterial adhesion and biofilm formation when used in an MFC.

2.6. Effect of Granular Volume on Power Generation

The optimal amount of granular material needed for use in the MFCs was investigated by using different granular volumes. This reflects the percentage of anode or cathode volume filled with granular material. Granular volumes were 40%, 25% and 15% of anode or cathode volume. These volumes correspond to masses of 57, 35 and 21 g respectively (Table 4). The granular volume could not be less than 10%, which caused rapid voltage fluctuations due to poor contact between granules and the stainless steel rod. It should also not exceed 45% to avoid electrolyte spillage.

Table 4. Basic properties of the layer of AC granules used in the MFCs of 2–4 mm in diameter and 0.57 g/cm^3 in bulk density.

Parameter	40 vol. % Granules	25 vol. % Granules	15 vol. % Granules
Mass of granules (g)	57	35	21
Projected surface area (m^2)	0.37	0.23	0.14
Granular bed height (mm)	36	27	17

The voltages generated by the three granular volumes were fairly similar with a deviation of $\pm$4 mV. The power densities relative to the projected electrode surface area were 1.18, 1.88 and 3.12 mW/m^2 for 40%, 25% and 15% granular volume, respectively. Power densities relative to the anode volume were 1.74, 1.71 and 1.70 W/m^3 for 40%, 25% and 15% granular volume, respectively. This indicates that with approximately three times less granular material the same amount of power can be generated relative to anode active volume (Figure 7). This further indicates that electrogenically active biofilm formation does not increase with increasing granular bed height. MFCs operating with AC can use as little as 15% granules of its anode or cathode volume and still attain significant power for use which enhances its scalability, cost-efficiency and sustainability.

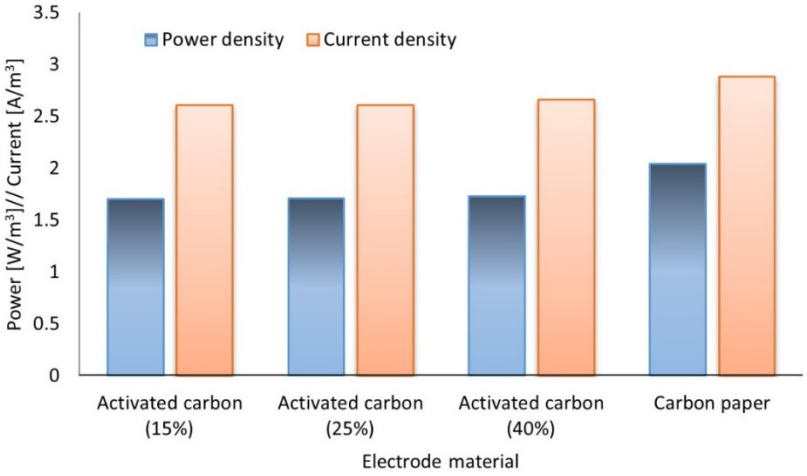

Figure 7. Performance of palm kernel shell AC (various granular volumes) relative to CP (standard) tested in an MFC.

2.7. Performance of AC Relative to CP

CP has been used globally in MFCs as electrode material for both anodes and cathodes. This made it a suitable material for standardization of AC. Under identical conditions of operation, MFCs operating with CP yielded 10%–15% higher power density (2.04 W/m^3) than with AC (1.73 W/m^3) (Table 5). This difference is appreciable even though AC possesses a much larger surface area than CP and is likely due to the more efficient electron transfer aided by strongly bonded carbon strands in CP providing excellent interconnected network (Figures 5a and 6a) in contrast with the inter-granular electron transfer in AC. Granules in AC have no binding agent and rely on direct physical contact between the granules for electron transfer. There are therefore significant losses due to the reliance on electron transfer from one granule to another until its final collection at the stainless steel rod. Nevertheless, the ease in preparation of AC compensates for these losses compared with the high cost of CP that requires advanced technology and high skills, which is appreciable.

Despite the finding that pyrolysis at 500 °C leads to a low degree of carbonization [21,22], the present study showed acceptable electricity generation with AC (Figure 2) and less internal resistance than with CP (Figure 3).

Table 5. Comparison of palm kernel shell AC and CP electrode performance obtained in the MFCs.

Electrode Material	Inoculum Used	Length of Start-up (Days)	Maximum Voltage Under Load (mV)	Power Density (mW/m^3)
CP	FS	6 ± 1	714 ± 10	2040 ± 55
	GW	3 ± 0.5	540 ± 26	1169 ± 110
AC	FS	6 ± 2	657 ± 9	1727 ± 47
	GW	4 ± 1	516 ± 7	1066 ± 32

3. Experimental Section

3.1. MFC Configuration

The H-shaped MFCs were constructed of two acrylic chambers with a volume of 300 mL, connected with an acrylic tube (Department of Chemical and Biochemical Engineering; Technical University of Denmark, Lyngby, Denmark) [25]. The reactor is presented by Sun *et al.* [31]. A proton exchange membrane (PEM; Nafion™ N117, Fuel Cell Earth LLC, Woburn, MA, USA) with an area of 7.1 cm^2 was placed between the chambers.

3.2. Inoculation

The first inoculum was FS from the Kumasi Metropolitan Assembly Landfill site, Ghana (6.6243° N, 1.5906° W). It was primarily composed of urine and fecal matter from public and private septic facilities. Samples were collected from the influent of the first stabilization pond. The second inoculum was GW from the wastewater treatment plant of the Kwame Nkrumah University of Science and Technology, Ghana (6.6650° N, 1.5734° W). It was primarily composed of water from laundries and washrooms. Samples were collected at the influent of the primary sedimentation tank.

The wastewater was used solely as inoculum but contributed with an amount of substrate, which was quantified and referred to as secondary substrate. The primary substrate was sodium acetate. The wastewater for inoculation was stored at room temperature to maintain the microbial activity and prevent selective microbial growth (through storage by freezing). The properties of FS were 7.2 ± 1.6 g/L COD, pH 8.2 ± 0.4, conductivity of 17.2 ± 2.4 mS/cm and 12.7 ± 1.6 g/L total solids. The properties of GW were 1.4 ± 0.2 g/L COD, pH 7.6 ± 0.4, conductivity of 1.4 ± 0.2 mS/cm and 1.1 ± 0.1 g/L total solids (Table 1).

3.3. Electrode Preparation

The electrode materials used were AC prepared from palm kernel shells, which were pretreated by washing, air-drying and screening to remove impurities. They were pyrolyzed at 500 °C for four hours and activated with steam at 130–165 °C for three hours to increase the active surface area. Oxygen was removed prior to the pyrolysis. Granules of AC were obtained by crushing and sieving to sizes of 2–4 mm in diameter from an initial size range of 10–25 mm. The AC granules were packed into the anode and cathode chambers as a granular bed around a stainless steel rod, which was used as current collector to the external circuit. CP sheets (Toray TGPH-20, Pemeas USA, Inc., E-TEK division, Somerset, NJ, USA) of 3 × 13 cm were used as baseline.

3.4. MFC Operation

The anode chamber was filled with the selected wastewater with COD concentration of 13.1 g/L COD for FS and 3.6 g/L COD for GW after adding the substrate (sodium acetate concentration of 3 g/L $C_2H_3NaO_2$ was added in both cases (equivalent to 3 × 64/82 = 2.3 g/L COD)). The anode chamber was sealed to create an anaerobic environment for bacterial growth. The cathode chamber was filled with 220 mL of 100 mM $K_3Fe(CN)_6$ solution exposed to atmospheric oxygen. The system was operated in fed-batch mode at ambient conditions (*i.e.*, temperature = 28 ± 3 °C). The experiments were conducted in duplicate with two reactors running at each of the conditions tested. The number of feeding cycles was four including the feeding cycle. The cycle length was eight days for the feeding cycle and six days for the subsequent cycles.

3.5. Microbial Analysis

Biofilm samples from the anode chamber were obtained from 0.5 cm^2 CP or four AC granules corresponding to 0.5 cm^2 surface at the end of cycle 3. Genomic DNA was extracted using the PowerBiofilm™ DNA Isolation Kit (MO-BIO, Carlsbad, CA, USA) according to the manufacturer's instructions [25]. DNA was amplified by polymerase chain reaction (PCR) in a C1000™ thermo-cycler (Bio-Rad, Hercules, CA, USA) as described by Muyzer *et al.* [15], using the primer 16S rDNA-338F containing a GC clamp and 16S rDNA-518R. DGGE was performed using the DCODE™ Universal Mutation Detection System (Bio-Rad, Hercules, CA, USA) and the resulting bands were identified based on standards published by Sun *et al.* [25].

3.6. SEM Microscopy

In order to examine biofilms on the anode electrode surfaces, the electrode (~2 cm^2) was removed without touching its surface. Samples were fixed in 3% v/v glutaraldehyde, +2% paraformaldehyde in

0.1 M Na-cacodylate buffer in deionized water (pH 7.2). After fixation, the samples were dehydrated in aqueous ethanol using: 20%, 40%, 60%, 80%, 90% and 100% for 15 min in each solution. Subsequent dehydration was performed in 33%, 66% and 100% acetone in ethanol before samples were critical point dried using an Agar E3000 critical point dryer (Agar Scientific, Stansted, Essex, UK) with liquid CO_2 as drying agent. Following coating with gold using an Emitech E5000 sputter coater, samples were observed using a Philips XL30 ESEM microscope at 50 to 10,000 magnification [25].

3.7. Analytical Methods

Conductivity was determined using a conductivity meter (VWR CO 310; VWR Int. Ltd., Leicestershire, UK) and COD determined with a chemical kit (Hanna COD kit: HI 939800, HI 93754-25, HI 83214; HANNA Instruments, Texas, TX, USA). The cell voltage across a 1000 Ω resistor was monitored every 10 s using a data logger (Pico Log ADC 20/24, Pico Technology Cambrigeshire, UK). The electrode surface area of the granules was calculated as a projected surface area (assuming spherical shape with a diameter of 3 mm). EIS was conducted using a potentiostat (Gamry G750, Gamry Instruments Inc., Warminster, PA, USA) to determine the internal resistance when the MFCs were at stable performance. For overall impedance the MFC was connected to the potentiostat in a two-electrode mode. The frequency range was 20 kHz to 0.1 Hz with amplitude of 0.3 mA and six points per decade.

4. Conclusions

Palm kernel shell AC was successfully inoculated in MFCs with fecal sludge and grey water producing appreciable steady state voltage and power density of 0.6 V and 1.73 W/m^3 in several post-inoculation cycles. SEM microscopy showed biofilm formation initiating oxidation of organic substrate for generation of electricity aided by nanowires. Granular volumes could be reduced to 15% of the anode chamber volume to optimize electrode based power densities. Since AC achieved power densities were comparable to CP, AC can be strongly considered as an electrode material for application in MFCs in tropical regions.

Acknowledgments: The authors are grateful to Anne S. Meyer and Guotao Sun for hosting and supporting Felix Offei in performing microbial analysis at Technical University of Denmark (DTU). The authors are also grateful to Danida Fellowship Centre for supporting the research project (Biobased electricity in developing countries, DFC No. 11–091 Risø). Finally Irina Skjødt, DTU is acknowledged for excellent accounting work on the project and the workshop at Department of Chemical and Biochemical Engineering, DTU, for excellent manufacture of the MFC reactors.

Author Contributions: All seven authors contributed substantially to the work. Felix Offei, Anders Thygesen and Moses Mensah designed experiments; Felix Offei and Kwame Tabbicca conducted the experiments and data analysis; Anders Thygesen and Moses Mensah supervised and interpreted the experimental work, Felix Offei and Anders Thygesen wrote the paper. Dinesh Fernando and Anders Thygesen prepared samples for SEM microscopy and performed SEM. Dinesh Fernando and Geoffrey Daniel checked the manuscript and prepared figures on the SEM microscopy part. Irina Petrushina and Anders Thygesen analyzed and interpreted the EIS data.

Conflicts of Interest: The authors declare no conflict of interest.

References

1. Thygesen, A.; Thomsen, A.B.; Possemiers, S.; Verstraete, W. Integration of microbial electrolysis cells (MECs) in the biorefinery for production of ethanol, H_2 and phenolics. *Waste Biomass Valor.* **2010**, *1*, 9–20. [CrossRef]
2. Liu, H.; Cheng, S.A.; Logan, B.E. Power generation in fed-batch microbial fuel cells as a function of ionic strength, temperature, and reactor configuration. *Environ. Sci. Technol.* **2005**, *39*, 5488–5493. [CrossRef] [PubMed]
3. Logan, B.E.; Hamelers, B.; Rozendal, R.; Schröder, U.; Keller, J.; Freguia, S.; Aelterman, P.; Verstraete, W.; Rabaey, K. Microbial fuel cells: Methodology and technology. *Environ. Sci. Technol.* **2006**, *40*, 5181–5192. [CrossRef] [PubMed]
4. Thygesen, A.; Angelidaki, I.; Min, B.; Poulsen, F.W.; Bjerre, A.B. Electricity generation by microbial fuel cells fuelled with wheat straw hydrolysate. *Biomass Bioenerg.* **2011**, *35*, 4732–4739. [CrossRef]

5. Ahn, Y.; Logan, B.E. Effectiveness of domestic wastewater treatment using microbial fuel cells at ambient and mesophilic temperatures. *Bioresour. Technol.* **2010**, *101*, 469–475. [CrossRef] [PubMed]
6. Nam, J.Y.; Kim, H.W.; Lim, K.H.; Shin, H.S. Effects of organic loading rates on the continuous electricity generation from fermented wastewater using a single-chamber microbial fuel cell. *Bioresour. Technol.* **2010**, *101*, 33–37. [CrossRef] [PubMed]
7. Aelterman, P.; Versichele, M.; Marzorati, M.; Boon, N.; Verstraete, W. Loading rate and external resistance control the electricity generation of microbial fuel cells with different three-dimensional anodes. *Bioresour. Technol.* **2008**, *99*, 8895–8902. [CrossRef] [PubMed]
8. Zhou, M.; Chi, M.; Luo, J.; He, H.; Jin, T. An overview of electrode materials in microbial fuel cells. *J. Power Sources* **2011**, *196*, 4427–4435. [CrossRef]
9. He, Z.; Minteer, S.D.; Angenent, L.T. Electricity generation from artificial wastewater using an upflow microbial fuel cell. *Environ. Sci. Technol.* **2005**, *39*, 5262–5267. [CrossRef] [PubMed]
10. Moon, H.; Chang, I.S.; Kim, B.H. Continuous electricity production from artificial wastewater using a mediator-less microbial fuel cell. *Bioresour. Technol.* **2006**, *97*, 621–627. [CrossRef] [PubMed]
11. Jiang, D.; Curtis, M.; Troop, E.; Scheible, K.; McGrath, J.; Hu, B.; Suib, S.; Raymond, D.; Li, B. A pilot-scale study on utilizing multi-anode/cathode microbial fuel cells (MAC MFCs) to enhance the power production in wastewater treatment. *Int. J. Hydrogen Energy* **2011**, *36*, 876–884. [CrossRef]
12. Jiang, D.; Li, B. Granular activated carbon single-chamber microbial fuel cells (GAC-SCMFCs): A design suitable for large-scale wastewater treatment processes. *Biochem. Eng. J.* **2009**, *47*, 31–37. [CrossRef]
13. Santoro, C.; Artyushkova, K.; Babanova, S.; Atanassov, P.; Ieropoulos, I.; Grattieri, M.; Cristiani, P.; Trasatti, S.; Li, B.; Schuler, A.J.; *et al*. Parameters characterization and optimization of activated carbon (AC) cathodes for microbial fuel cell application. *Bioresour. Technol.* **2014**, *163*, 54–63. [CrossRef] [PubMed]
14. Pant, D.; Van Bogaert, G.; De Smet, M.; Diels, L.; Vanbroekhoven, K. Use of novel permeable membrane and air cathodes in acetate microbial fuel cells. *Electrochim. Acta* **2010**, *55*, 7710–7716. [CrossRef]
15. Muyzer, G.; de Waal, E.C.; Uitterlinden, A.G. Profiling of complex microbial populations by denaturing gradient gel electrophoresis analysis of polymerase chain reaction-amplified genes coding for 16S rRNA. *Appl. Environ. Microbiol.* **1993**, *59*, 695–700. [PubMed]
16. Dong, H.; Yu, H.; Wang, X.; Zhou, Q.; Feng, J. A novel structure of scalable air-cathode without nafion and pt by rolling activated carbon and PTFE as catalyst layer in microbial fuel cells. *Water Res.* **2012**, *46*, 5777–5787. [CrossRef] [PubMed]
17. Chen, S.; He, G.; Hu, X.; Wang, S.; Zeng, D.; Hou, H.; Schroder, U. A three dimensional ordered macroporous carbon derived from a natural plant resource as anode for microbial bioelectrochemical systems. *ChemSusChem* **2012**, *5*, 1059–1063. [CrossRef] [PubMed]
18. Chen, S.; He, G.; Liu, Q.; Harnisch, F.; Zhou, Y.; Chen, Y.; Hanif, M.; Wang, S.; Peng, X.; Hou, H.; *et al*. Layered corrugated electrode macrostructures boost microbial bioelectrocatalysis. *Energy Environ. Sci.* **2012**, *5*, 9769–9772. [CrossRef]
19. Palm Biomass Burning Oil Palm Products. Available online: http://oilpalmproducts.com (accessed on 4 January 2016).
20. Abechi, S.E.; Gimba, C.E.; Uzairu, A.; Dallatu, Y.A. Preparation and characterization of activated carbon from palm kernel shell by chemical activation. *Res. J. Chem. Sci.* **2013**, *3*, 54–61.
21. Yacob, A.B.; Wahab, N.; Suhaimi, N.H.; Amat, M.K.A. Microwave induced carbon from waste palm kernel shell activated by phosphoric acid. *Int. J. Eng. Technol.* **2013**, *5*, 214–217. [CrossRef]
22. Herawan, S.G.; Hadi, M.S.; Ayob, R.; Putra, A. Characterization of activated carbons from oil-palm shell by CO_2 activation with no holding carbonization temperature. *Sci. World J.* **2013**, *1*, 1–6. [CrossRef] [PubMed]
23. Logan, B.E.; Murano, C.; Scott, K.; Gray, N.D.; Head, I.M. Electricity generation from cysteine in a microbial fuel cell. *Water Res.* **2005**, *39*, 942–952. [CrossRef] [PubMed]
24. Sun, G.; Rodrigues, D.S.; Thygesen, A.; Daniel, G.; Fernando, D.; Meyer, A.S. Inocula selection in microbial fuel cells based on anodic biofilm abundance of *Geobacter sulfurreducens*. *Chin. J. Chem. Eng.* **2016**, in press. [CrossRef]
25. Sun, G.; Thygesen, A.; Meyer, A.S. Acetate is a superior substrate for microbial fuel cell initiation preceding bioethanol effluent utilization. *Appl. Microbiol. Biotechnol.* **2015**, *99*, 4905–4915. [CrossRef] [PubMed]
26. Yuan, X.Z.; Song, C.; Wang, H.; Zhang, J. *Electrochemical Impedance Spectroscopy in PEM Fuel Cells*; Springer-Verlag London Ltd.: London, UK, 2010.

27. Marzorati, M.; Wittebolle, L.; Boon, N.; Daffonchio, D.; Verstraete, W. How to get more out of molecular fingerprints: Practical tools for microbial ecology. *Environ. Microbiol.* **2008**, *10*, 1571–1581. [CrossRef] [PubMed]
28. Thygesen, A.; Marzorati, M.; Boon, N.; Thomsen, A.B.; Verstraete, W. Upgrading of straw hydrolysate for production of hydrogen and phenols in a microbial electrolysis cell (MEC). *Appl. Microbiol. Biotechnol.* **2011**, *89*, 855–865. [CrossRef] [PubMed]
29. Bond, D.R.; Lovley, D.R. Electricity production by *Geobacter sulfurreducens* attached to electrodes. *Appl. Environ. Microbiol.* **2003**, *69*, 1548–1555. [CrossRef] [PubMed]
30. Reguera, G.; Nevin, K.P.; Nicoll, J.S.; Covalla, S.F.; Woodard, T.L.; Lovley, D.R. Biofilm and nanowire production leads to increased current in *Geobacter sulfurreducens* fuel cells. *Appl. Environ. Microbiol.* **2006**, *72*, 7345–7348. [CrossRef] [PubMed]
31. Sun, G.; Thygesen, A.; Ale, M.T.; Mensah, M.; Poulsen, F.W.; Meyer, A.S. The significance of the initiation process parameters and reactor design for maximizing the efficiency of microbial fuel cells. *Appl. Microbiol. Biotechnol.* **2014**, *98*, 2415–2427. [CrossRef] [PubMed]